Multiphoton Dissociation and Ionization of Metallocenes Cooled in Supersonic Beams

Samuel Leutwyler,[†] Uzi Even, and Joshua Jortner*

Department of Chemistry, Tel-Aviv University, Tel-Aviv, Israel (Received: July 28, 1981)

Multiphoton dissociation/ionization of ferrocene and nickelocene was studied in effusive and in supersonic molecular beams. Mass spectrometric ion detection revealed almost exclusive generation of bare metal ions, both by resonant and by nonresonant mechanisms.

Introduction

Recent work[1-4] on the gas-phase photophysics of organometallic compounds with pulsed, tunable, high-fluence lasers has provided evidence for unusually strong multiphoton processes in these molecules, involving (a) multiphoton dissociation (MPD) by sequential absorption of several vis/UV photons to yield the free metal atom (plus ligands), followed by (b) resonant multiphoton ionization (MPI) of the metal atoms at wavelengths corresponding to atomic one-photon or two-photon resonant absorptions.

Previous work on metallocenes[1,2] and metal carbonyls[2,3] in ionization cells explored MPD/MPI processes in gaseous samples at room temperature and pressures of 0.005-1 torr.[1-3] While the identification of resonant atomic MPI rested on the assignment of atomic resonances, unstructured continuous ion signals were also observed, in both the carbonyls and metallocenes, for which only tentative assignments were given. The role of collisional processes in MPD/MPI is also not yet clearly defined; while in the short-pulse/low-pressure experiments (5 × 10⁻⁹ s/0.005 torr)[1] the MPD/MPI processes are believed to be truly intramolecular, proceeding without collisional assistance, on the other hand, strong collisional enhancement was noted for long-pulse experiments (1 μs) on ferrocene at 1 torr.[2]

Pioneering MPD/MPI work in molecular beams was undertaken by Smalley and co-workers[4] on mononuclear metal carbonyls ($Fe(CO)_5$, $Cr(CO)_6$, $Mo(CO)_6$). They found a spectrally diffuse dependence of photoion production with no characteristic atomic transitions in contrast to the bulb studies.[1-3] We believe that the different experimental conditions (high laser intensities and fluxes) employed by Smalley et al.[4] may be responsible for the erosion of spectral structure. The ultrahigh ionization efficiency reported (close to 100%)[4] indicates that most or all of the photon absorption steps were saturated, and spectral structure was therefore lost, presumably due to power broadening.

We have undertaken a study of the MPD/MPI processes in nickelocene and ferrocene, using molecular beam techniques together with mass spectrometric detection of the ions formed, in an attempt to answer the following questions:

(a) Does laser-induced MPD/MPI of organometallics proceed in a true collision-free manner?

(b) Can the resonant atomic lines be ascribed exclusively to production of the bare metal ion?

(c) What is the nature and composition of the continuous ion background signal?

(d) Are MPD/MPI processes influenced by the internal energy content of the molecule, i.e., can the MPI spectra be changed by cooling in supersonic jets?

Experimental Section

The experimental setup including data collection has been previously described.[5]

Metallocene molecular beams were produced in two different source arrangements, in order to detect temperature effects: as thermal, effusive beams, where the metallocenes at their room temperature vapor pressure of 0.005-0.01 torr were allowed to effuse through the TOF mass spectrometer ion source out of a stainless-steel capillary ($\phi = 0.6$ mm), and as seeded supersonic beams, where the metallocenes (at vapor pressures of 0.05-0.2 mbar) were seeded into Ar carrier gas at stagnation pressures of $5 < p_0 < 200$ mbar and expanded through a stainless-steel nozzle ($\phi = 180$ μm). Supersonic expansion of large aromatic molecules seeded into a similar stagnation pressures of Ar is known to result in terminal beam vibrational temperatures $T_{vib} \approx 10$ K and rotational temperatures $T_{rot} < 10$ K.[6]

A N_2-laser-pumped dye-laser system (Molectron UV-12/DL 14) was used to probe the metallocene MPD/MPI spectra. Typical output energies in the wavelength range 3800-5000 Å were 60-120 μJ/pulse in a pulse of ~4 ns (fwhm) with a bandwidth of 0.8 cm⁻¹. The laser radiation was focused into the center of the molecular beam inside the source region of the TOF mass spectrometer, at right angles to both the beam and time-of-flight (TOF) mass spectrometer axes. Photoions generated by laser-induced MPD/MPI were accelerated out of the ionization region to a final energy of 2000 V, using a double-field focusing arrangement. MPD/MPI signals could be obtained for a given ion as a function of laser wavelength, or, conversely, the total mass spectrum was measured for a fixed laser wavelength. A detailed description of the TOF spectrometer is given elsewhere.[7]

Results and Discussion

Typical wavelength dependences of metal ion production (Fe^+, Ni^+) from metallocenes by laser-induced MPD/MPI is shown in Figures 1 and 2 for ferrocene and nickelocene, respectively. The observation of Fe^+ and Ni^+ ions generated within single laser pulses in a collision-free regime confirms our previous assignment of the MPD/MPI processes as truly intramolecular. The metal ions were unambiguously identified by their isotopic mass peak pat-

(1) S. Leutwyler, U. Even, and J. Jortner, *Chem. Phys. Lett.*, 74, 11 (1980); *Chem. Phys.*, 58, 409 (1981).
(2) P. C. Engelking, *Chem. Phys. Lett.*, 74, 207 (1980).
(3) D. P. Gerrity, L. J. Rothberg, and V. Vaida, *Chem. Phys. Lett.*, 74, 1 (1980).
(4) M. A. Duncan, T. G. Dietz, and R. E. Smalley, *Chem. Phys.*, 44, 415 (1979).
(5) S. Leutwyler and U. Even, *Chem. Phys. Lett.*, 81, 578 (1981).
(6) A. Amirav, U. Even, and J. Jortner, *Chem. Phys.*, 51, 31 (1980).
(7) S. Leutwyler and U. Even, to be published.

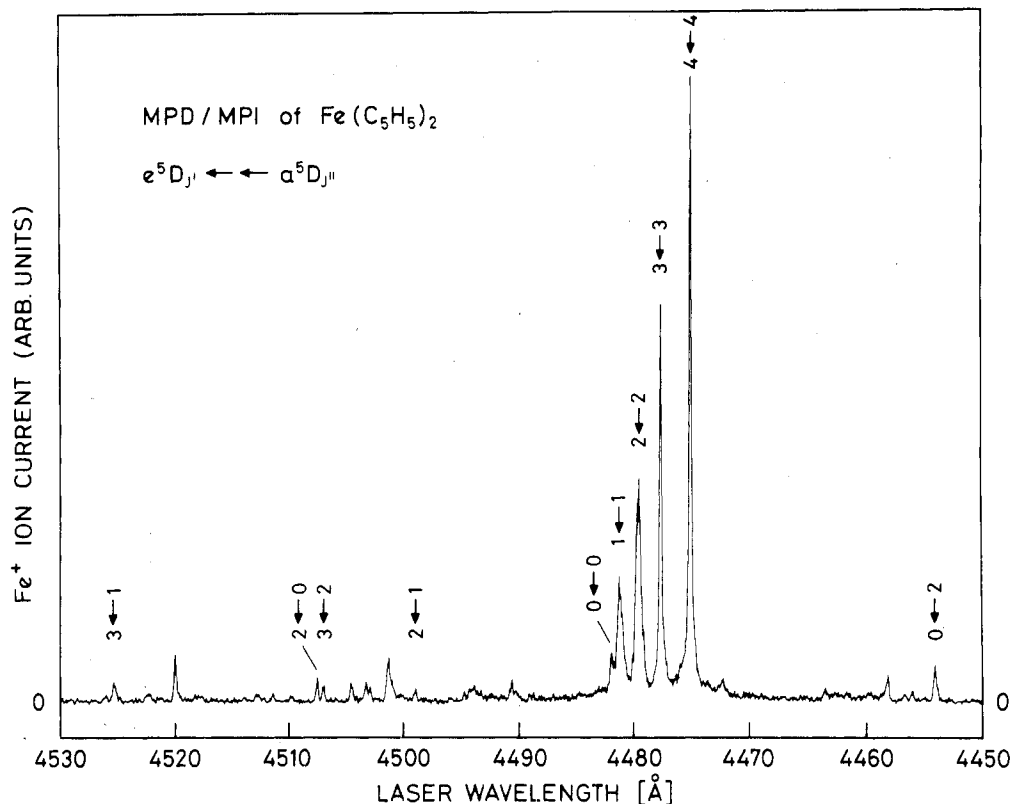[†]Physikalisch-Chemisches Institut, Universität Basel, CH-4056 Basel, Switzerland.

Figure 1. Wavelength dependence of the $^{56}Fe^+$ ion current produced by pulsed laser MPD/MPI of ferrocene in the λ_{air} = 4450–4530-Å range. The dominating feature is the two-photon resonant $e^5D \leftarrow \leftarrow a^5D$ multiplet with $J' = J''$. Several transitions between the same electronic terms with $\Delta J = \pm 1, \pm 2$ are noticeable, but show less intensity. Note the absence of nonresonant background ion signal.
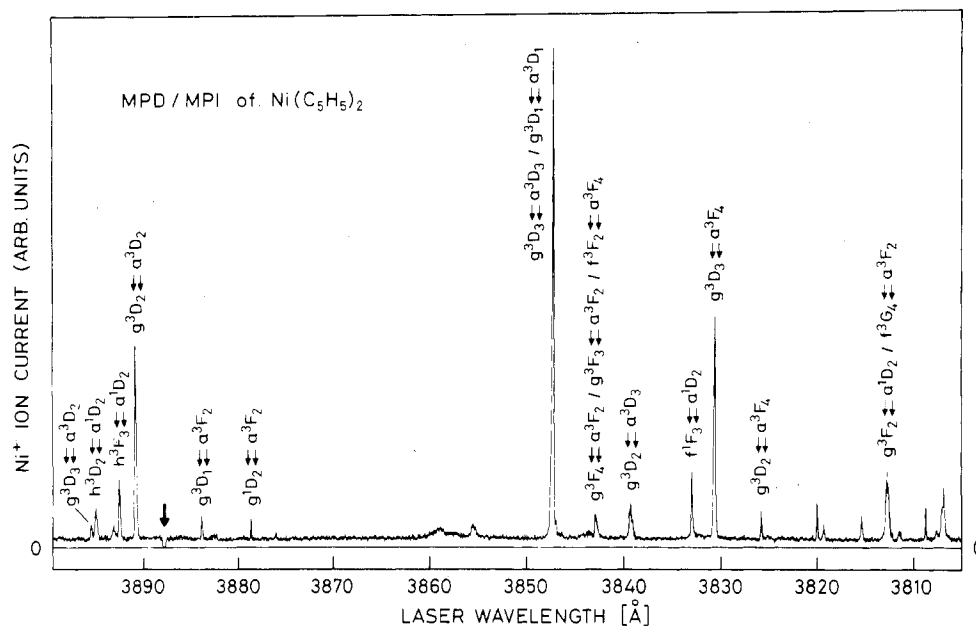

Figure 2. Wavelength dependence of the Ni^+ ion current (all isotopes) produced by collision-free laser MPD/MPI of nickelocene in the near-UV. Several peaks exhibit coincidental overlapping of different two-photon transitions and are multiply assigned. Note the genuine nonresonant background ion current with structure between 3855 and 3860 Å. The laser light was blocked at 3887.5 Å (indicated by arrow).

terns.[8] Comparison of spectra taken in the beam and in the ionization cell (at pressures ≤ 0.1 torr) show agreement in all important features, such as spectral position and relative intensities of atomic one- and two-photon resonant lines, as well as relative intensity of nonresonant background signal. As expected from the previous optical as-

signments, ion production at all resonant atomic lines yields exclusively the metal ions (abundance of other ions is less than 0.01% of the total ion current). Quite unexpectedly, ion production throughout the continuous nonresonant background region is also almost wholly due to the bare Fe^+ and Ni^+ ions.

Peak-to-background ratios were checked throughout the 3800–4000-Å wavelength region (photon energies 3.3–3.1 eV) in nickelocene (see Figure 2), and found to be close

(8) R. C. Weast, Ed., "Handbook of Chemistry and Physics", CRC Press, Cleveland, 1974, pp B 256-8.

TABLE I: Ion Abundances for the Nonresonant Laser MPD/MPI of Nickelocene[a]

| m/e	ion	abundance, %
12	C^+	1.9
24	C_2^+	1.0
36	C_3^+	0.65
39	$C_3H_3^+$	3.0
58–64	Ni^+	92.4
97–103	$NiC_3H_3^+$	0.28
123–129	$NiC_5H_5^+$	0.40
188–194	$NiC_{10}H_{10}^+$	0.54

[a] Laser wavelength: 3847.9 Å (3.222 eV); average laser fluence: 0.26 J cm^{-2}; average laser intensity: 6.5 × 10^7 W cm^{-2}.

or equal to those of the ionization cell measurements. Quite generally, ions other than the metal cation are produced at very low abundance; typical values for the nickelocene 3800–4000-Å background ion production region are given in Table I.

Cooling of the metallocenes in supersonic jets did not result in significant changes in the MPD/MPI spectra. The 3800–3900-Å region in ferrocene, which shows many resonant peaks as well as structured background, was studied as a function of stagnation pressure. The only change on increasing p_0 from 5 to 200 mbar was an overall reduction of the absolute signal strength to 30–50% of the low-pressure value; no significant changes in either resonance lines or background were observed. This result leads to the conclusion that absorption of the first photon in the neutral molecule term manifold is spectrally diffuse and structureless even at low temperatures. Absorption spectra of metallocenes in glassy matrices and solution show that the visible and near-UV absorption bands of nickelocene and ferrocene are weak (ϵ_{max} = 100) and diffuse, even at low temperature,[9,10] the electronic transitions being largely localized within the metal atom 3d levels and hence essentially symmetry forbidden. Intensity is gained via a vibronic coupling mechanism, which is characterized by a temperature-dependent oscillator strength.[11] On cooling in glassy matrices, band intensities are reduced, but band shapes change only slightly.[9,10] This is in excellent agreement with the cooling behavior of the MPD/MPI ion signals exhibited in the supersonic beam, which show no improvement in spectral resolution, but an overall signal reduction.

The nature of the intramolecular processes leading to nonresonant production of the bare metal ions will now be discussed.

Nickelocene. The nonresonant Ni$^+$ signal rises rather sharply at 3930 ± 10 Å by a factor of 20; previously, the background ion signal was assigned to molecular two-photon ionization, giving an ionization potential of 6.29 ± 0.015 eV:[1]

$$Nicp_2 \xrightarrow{\hbar\omega} \xrightarrow{\hbar\omega} Nicp_2^+ \quad (cp = C_5H_5) \qquad (1)$$
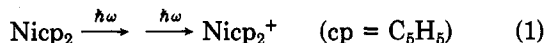
The adiabatic ionization potential as measured by Rabalais et al.[12] using photoelectron spectroscopy yields (IP(adiabatic) = 6.2 eV). This near coincidence lends strong support to the idea that the nonresonant Ni$^+$ signal ori-
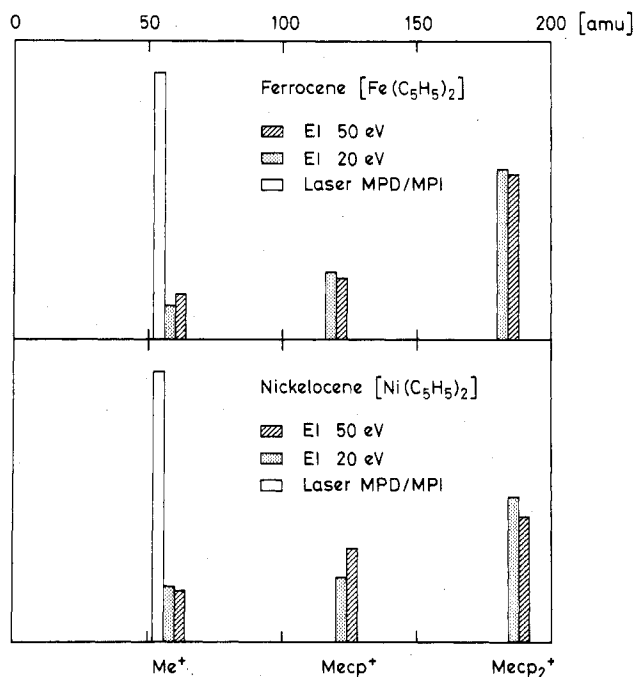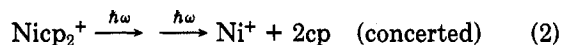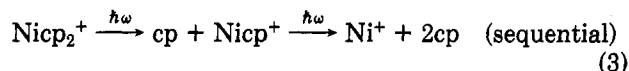

Figure 3. A comparison of normalized mass spectra of metallocenes as obtained by laser MPD/MPI and by electron impact at two different electron energies.[13,14]

ginates through molecular photoionization, eq 1, followed by molecular-ion photodissociation:

$$Nicp_2^+ \xrightarrow{\hbar\omega} \xrightarrow{\hbar\omega} Ni^+ + 2cp \quad (concerted) \qquad (2)$$

or

$$Nicp_2^+ \xrightarrow{\hbar\omega} cp + Nicp^+ \xrightarrow{\hbar\omega} Ni^+ + 2cp \quad (sequential) \qquad (3)$$

or

$$Nicp_2^+ \xrightarrow{\hbar\omega} \xrightarrow{\hbar\omega} Ni^+ + fulvalene \quad (rearrangement) \qquad (4)$$

The energy uptake in molecular-ion photodissociation for processes 2 and 3 is given by

$$E_{diss}(Nicp_2^+) = IP(Ni) + E_{diss}(Nicp_2) - IP(Nicp_2) \qquad (5)$$

For the calorimetric value of $E_{diss}(Nicp_2)$,[13] the resulting $E_{diss}(Nicp_2^+)$ is 6.3 ± 0.4 eV, indicating that ion photodissociation may proceed by absorption of 2–3 near-UV photons. The dissociation–rearrangement process (reaction 4) would require a smaller energy uptake. The absorption spectrum of the nickelocenium cation has been reported by Traverso and Rossi[16] and by Borrell and Henderson.[17] The experimental spectra show two broad electronic transitions of moderate intensity (ϵ = 700–1500) located in the spectral region of interest (3.1–3.3 eV). On the other hand, the absorption cross sections of the neutral nickelocene molecule are low (ϵ_{max} < 200 for energies < 3.3 eV) and thus lower than the molecular-ion cross sections by almost one order of magnitude. In this situation, absorption in the neutral term manifold kinetically limits the multiphoton up-pumping process; also, for increasing laser

(9) A. T. Armstrong, F. Smith, E. Elder, and S. P. McGlynn, *J. Chem. Phys.*, **46**, 4321 (1967).

(10) I. Pavlik, V. Cerny, and E. Maxova, *Collect. Czech. Chem. Commun.*, **35**, 3045 (1980).

(11) E. S. Pysh, J. Jortner, and S. A. Rice, *J. Chem. Phys.*, **40**, 2018 (1964).

(12) J. W. Rabalais, L. O. Werme, T. Bergmark, L. Karlsson, M. Hussain, and K. Siegbahn, *J. Chem. Phys.*, **57**, 1185 (1972).

(13) H. A. Skinner in "Advances in Organometallic Chemistry", Vol. 2, F. G. A. Stone and R. West, Ed., Academic Press, New York, 1964, p 49.

(14) E. Schumacher and R. Taubenest, *Helv. Chim. Acta*, **47**, 1525 (1964).

(15) L. Friedman, A. P. Irsa, and G. Wilkinson, *J. Am. Chem. Soc.*, **77**, 3689 (1955).

(16) O. Traverso and R. Rossi, *Ann. Univ. Ferrara, Sez. 5*, **3**, 167 (1974).

(17) P. Borrell and E. Henderson, *Inorg. Chim. Acta*, **12**, 215 (1975).

intensity, the absorption steps in the ionic manifold will be saturated before the absorption steps in the neutral manifold. In this case the intensity dependence measured[1] for the nonresonant background between 3.1 and 3.3 eV, with exponent n = 2–3, does not reflect the true order of the process, but sets a lower limit to the total photon uptake. The total number of 3.1–3.3-eV photons necessary to generate Ni^+ from $Nicp_2$ is at least four (see above and ref 1), in agreement with the mass spectrometric appearance potential $(AP(Ni^+) = 13.6 eV)$.

Ferrocene. The nonresonant ion background signal was also found to be almost exclusively due to Fe^+. The analysis is, however, characteristically different from that of nickelocene in several respects: the nonresonant background is strongly structured and extends from 3750 to 4200 Å (3.3 – 2.95 eV); as the adiabatic ionization potential of ferrocene is 6.72 eV,[9] two-photon molecular photoionization is not possible for photon energies up to 3.3 eV. On the other hand, uptake of two photons is sufficient to induce at least partial dissociation:

$$Fecp_2 \xrightarrow{\hbar\omega} \xrightarrow{\hbar\omega} Fecp + cp \qquad (6)$$

Nonresonant production of Fe^+ hence probably proceeds through the Fecp intermediate.

A comparison of mass spectra obtained by electron impact (EI) at electron energies of 20[14] and 50 eV[15] and those obtained by laser MPD/MPI is shown in Figure 3. The amount of energy transferred to the molecular system on electron impact is not well-known and is represented by a broad distribution (the "deposition function"); however, the two EI mass spectra show very similar fragmentation patterns, despite the large difference in electron energies. The laser MPD/MPI mass spectrum is qualitatively completely different, reflecting the multitude of dissociation and predissociation processes occurring when energy is delivered to the molecule in quanta which are commensurate with metal–ligand bond energies but smaller than the molecular ionization potential.

In conclusion, we summarize the main points of this study as follows: (a) confirmation of the collision-free, truly intramolecular nature of laser MPD/MPI processes in metallocenes; (b) unequivocal identification of the ions produced, being almost exclusively the metal ions Fe^+ and Ni^+, both at atomic resonances as well as throughout the nonresonant ion background signal region; (c) independence of the MPD/MPI spectra on cooling in supersonic jets, indicating that the first absorption step is truly diffuse, even at very low temperatures. Clarification of laser MPD/MPI processes in metallocenes have shown them to be a unique pulsed, efficient, intense, room-temperature source of pure metal ions in the gas phase. An obvious multitude of applications in gas-phase ion physics and ion chemistry can be foreseen.

Latent Heat of Vaporization of a Fluid

S. Torquato

Department of Mechanical Engineering, General Motors Institute, Flint, Michigan 48502

and G. Stell*

Departments of Mechanical Engineering and Chemistry, State University of New York at Stony Brook, Long Island, New York 11794
(Received: August 7, 1981)

Renormalization-group theory is applied to obtain the functional form of the latent heat of vaporization of a pure fluid that is applicable throughout the entire domain of existence of latent heat. To illustrate the use of the latent-heat expression, we least-squares fit it to latent-heat data of water.

We apply the results of renormalization-group theory to obtain a functional form of the latent heat of vaporization L of a pure fluid that is applicable throughout the entire domain of existence of the latent heat, i.e., from the triple point to the critical point. The resulting formula for the latent heat contains system-dependent parameters which ultimately must be fitted to data.

The latent heat of a fluid may be written as a sum of two parts: one being the contribution to L describing the singular behavior near the critical point and the other being the analytic or regular contribution to L characterizing the behavior away from the critical region. Ley-Koo and Green[1] made use of the general form of the singular part of the thermodynamic potential proposed by Wegner[2] for describing the critical region of fluids. Employing their expression in conjunction with the Clausius–Clapeyron equation, we are motivated to write

$$L = a_1 t^\beta + a_2 t^{\beta+\Delta} + a_3 t^{1-\alpha+\beta} + \sum_{n=1}^{M} b_n t^n \qquad (1)$$

where the first three terms account for behavior in the vicinity of the critical point and the finite sum describes

(1) Ley-Koo, M.; Green, M. S. *Phys. Rev. A* 1977, *16*, 2483; 1981, *23*, 2650.

(2) Wegner, F. J. *Phys. Rev. B* 1972, *5*, 4529. The precise values of α and β are still open to some uncertainty. Our fractions, which fall well within the range of currently reasonable values, were chosen for their simplicity and convenience. In particular, for $\beta = 1/3$, the term constant $\times t^{3\beta}$, which is a singular term found in ref 1, coincides with our lowest-order regular term, $b_1 t$. The value of Δ is not well established either experimentally or theoretically; 1/2 from lowest-order theoretical calculations is the most commonly used value. We determine it here by a least-squares fit of data.